NASA Technical Memorandum 89857
AIAA-87-1060

Arcjet Component Conditions Through a Multistart Test

Frank M. Curran and Thomas W. Haag
Lewis Research Center
Cleveland, Ohio

Prepared for the
19th International Electric Propulsion Conference
cosponsored by the AIAA, DGLR, and JSASS
Colorado Springs, Colorado, May 11-13, 1987

NASA

ARCJET COMPONENT CONDITIONS THROUGH A MULTISTART TEST

Frank M. Curran and Thomas W. Haag

National Aeronautics and Space Administration
Lewis Research Center
Cleveland, Ohio 44135

Abstract

A low power, dc arcjet thruster was tested for starting reliability using hydrogen-nitrogen mixtures simulating the decomposition products of hydrazine. More than 300 starts were accumulated in phases with extended burn-in periods interlaced. A high degree of flow stabilization was built into the arcjet and the power supply incorporated both rapid current regulation and a high voltage, pulsed starting circuit. A nominal current level of 10 A was maintained throughout the test.

Photomicrographs of the cathode tip showed a rapid recession to a steady-state operating geometry. A target of 300 starts was selected, as this represents significantly more than anticipated (150 to 240), in missions of 10 yr or less duration. Weighings showed no apparent mass loss. Some anode erosion was observed, particularly at the entrance to the constrictor. This was attributed to a brief period during startup that the arc anode attachment point spends in the high pressure region upstream of the nozzle.

Based on the results obtained, startup does not appear to be performance or lifelimiting for the number of starts typical of operational satellite applications.

E-3525

Introduction

Arcjet thrusters have long been considered for use in spacecraft propulsion. Research and development efforts first began in the mid 1950's and continued for approximately the next 10 years.[1] During this time the availability of nuclear electric power was assumed (SNAP-8 program) and the arcjet was seen mainly as a high thrust option for missions on which primary propulsion was required.[2] Because of this, most of the research was focussed on the 30 kW power level.[3-6] Government sponsored programs at the Plasmadyne Corporation did produce thrusters that ran at the 1 and 2 kW levels on hydrogen.[7-9] Recently, renewed interest in the arcjet has resulted in new programs for the advancement of arcjet technology.

While the 30 kW power level is still of interest,[10,11] much of the NASA research effort is centered on developing a unit capable of operating on storable propellants at power levels currently available on communications satellites ($P_e \leq 1.5$ kW). Ongoing research has shown that specific impulse levels in the 400 to 500 sec range are readily attainable. This is a significant increase over the current resistojet technology which is limited to a maximum of about 380 sec specific impulse, on hydrazine, by materials capabilities. The anticipated revenue enhancements that arcjet performance levels could provide have caused a considerable amount of discussion of requirements for a near term flight test.[12] Major efforts required prior to such a test include: (1) the development of an efficient flight-type power processor; (2) design, testing, and integration of an arcjet system that will operate over the range of power levels and blowdown pressures available on communications satellites; (3) completion of an impacts assessment study including the effects of radiated and conducted EMI and the effects on transmission through the arcjet plume; (4) extended duration life testing under true mission conditions and (5) development of a reliable procedure for starting the arcjet and affecting the transfer to steady state.

The need for this last effort was shown in early studies at NASA Lewis Research Center. In these, a Plasmadyne engine, left over from the SERT I program, was slightly modified and run with hydrogen-nitrogen mixtures simulating hydrazine and ammonia. A ballasted power supply with no high speed current regulation was used in these tests. Serious damage was incurred as the arcjet often remained in the low mode, in which the arc seats in the high pressure region upstream of the nozzle, for extended periods of time.[13,14] Improved starting was achieved on a short-term basis by incorporating stronger flow stabilization into the arcjet design and using an improved power processing unit.[15] This was an important advance, as missions proposed for arcjet application on communications satellites will probably require on the order of 200 on/off cycles for N-S station keeping and many more if the thruster is used for E-W station keeping and/or attitude control.

Starting phenomena continue to receive a high level of emphasis. As a next logical step on the path to a flight ready arcjet system a 300 start reliability test was performed. In this test, starts were performed before the thruster had been run for any appreciable amount of time, after brief duration firing, and after the thruster had been fully "burned-in." While the test successfully demonstrated more than 300 starting sequences, a number of phenomena were observed that bear further study. This report documents some of these phenomena and presents a photographic history of the electrodes before, during, and after the test. More details of the test can be found in a companion report.[16]

Apparatus

Arcjet Thruster

A cross-sectional schematic of the arcjet thruster used in the tests described herein is shown in Fig. 1(a). The cathode was a 3.2 mm diameter, 2 percent thoriated tungsten rod. Both the front and the rear insulators were made from boron nitride with calcium added to stabilize the boric acid binder and raise its melting point. A modified stainless steel gas fitting was used as a feed-through and to clamp the cathode in place. A threaded holding bolt inserted into the rear insulator from the opposite direction held the modified fitting in place. A piece of tantalum foil was

inserted between the front insulator and the cathode to center the cathode and to minimize gas flow around it. The anode housing was made of 316 stainless steel. A stainless steel fitting was threaded through this to serve as the propellant inlet. The anode insert was machined from 2 percent thoriated tungsten stock. The half angle on the chamber (converging) side of the insert was 30° while the nozzle itself was conical with a half angle of 20°. The constrictor was 0.64 mm (0.025 in.) in diameter and 0.25 mm (0.010 in.) in length. The nozzle area ratio was approximately 150. Vortex flow stabilization was provided by a stainless steel gas injection disk that fit between the front insulator and the upstream face of the anode insert. This injection disk had two circular, offset propellant feed passages, nominally 0.25 mm in diameter, to bring gas tangentially to the arc chamber, as shown in Fig. 1(b). Raised rings were machined into the upstream faces of both the injection disk and the anode insert. Grafoil gaskets placed over these rings affected a gas-tight seal when the front insulator was pushed forward by an inconel spring. This spring was compressed by the anode housing and the rear insulator which were held together by two stainless steel clamping plates secured by four bolts.

Power Supply

A pulse width-modulated power supply designed and built at NASA Lewis was used throughout the study[15]. This supply was capable of operating at up to 12 A at 140 V. A starting circuit was provided as an integral part of the power processor. This provided a high voltage pulse every second until arc ignition occurred. A typical starting pulse, from open circuit, is shown in Fig. 2. The pulses were approximately 4 kV in magnitude and 3 m/sec full width at half the maximum voltage. A fast storage oscilloscope was used to monitor starting transients at various points in the test. The voltage required for breakdown was typically between 1 and 3 kV. After breakdown two different phenomena were observed. In some starts the breakdown was followed by a transition to the steady state mode. In others, breakdown was followed by a substantial voltage oscillation (0 to 500 V). Examples of these are shown in Figs 3(a) and 3(b). Further study and discussion of the breakdown phenomena is presented elsewhere.[16] The oscillations were too rapid to be observed on the data recording system.

Vacuum Facility

Two vacuum facilities were used in these experiments. The first was a 1.5 m diameter by 5 m long vacuum chamber.[13] Under normal operating conditions, with the maximum flow rate of 4.3×10^{-5} kg/sec, the background pressure in this facility was less than 0.65 Pa (5×10^{-4} Torr). The second facility used was a bell jar which was 0.457 m in diameter and 0.61 m high. This was mounted on a 0.178 m high spool piece of the same diameter. Pumping was provided by a large roughing pump (20,700 SLPM). With no flow into the chamber the ambient pressure was approximately 45 Pa (0.35 Torr) while at the maximum gas flow rate the background pressure rose to about 90 Pa (0.65 Torr). The arcjet was mounted from the upper flange with the exhaust directed toward a water cooled stainless steel target. The electrical connections and the propellant feed line were also made through the top flange so that the entire flange could be lifted for easy access to the arcjet assembly. A photograph of this facility is shown in Ref. 16.

Thrust Measurement

The thrust measurement system used in the tests is described elsewhere.[16] Briefly, the thruster was mounted on a thermally isolated platform affixed to a second water-cooled platform supported on flexures. A linear variable differential transducer (LVDT) was used to measure platform displacements, from which applied thrust could be deduced. Known weights attached to a monofilament line attached to a windlass and the thruster platform were used for calibration. The entire apparatus, with the exception of the arcjet, was surrounded by a water cooled copper jacket. This arrangement virtually eliminated thermal drift in that the thruster could be run for hours with no detectable offset observed in the thrust measurement.

Flow Control and Metering

Different flow control systems were used in the two facilities. In the larger facility commercially available flowmeters employing thermal conductivity type sensors were used. These had a full scale range of 5 SLPM and were calibrated in-situ. The propellant feed system was designed to allow use of hydrogen, nitrogen or mixtures of the two. Stainless steel valves employing bellows seals were used for on/off control, while precision needle valves were utilized to adjust the propellant flows. The bell jar system was equipped with commercially available mass flow controllers. A central power supply and readout unit ran individual controllers for both hydrogen and nitrogen. The controllers were designed and factory calibrated for the specific gases and also were calibrated in situ. As on the other system, the gases could be mixed on the propellant flow panel. For this system no needle valves were necessary as the flow controllers actively maintained the propellant flow rates at preset levels.

Data Recording

An eight channel brush recorder was used to record current, voltage, thrust, propellant flow rate and pressure readings. The individual channels were isolated from each other and each was isolated from input to output via internal isolation transformers. It was found during the test that the voltage channel did, at times, induce noise into the other channels. To prevent this an additional isolation amplifer was added. An analog storage oscilloscope with differential inputs was used to monitor starting phenomena on the microsecond time scale.

Power Metering

Power was monitored by measuring the arc current and voltage levels. The voltage measurements were taken at the point where the power leads fed through the flange into the vacuum chamber. The current was sensed with a Hall-effect current probe.

Experimental Procedures

All starts were taken with the power supply set at a nominal value of 10 A. For the purposes of this study a start is defined as the breakdown and the subsequent transfer to stable, diffuse arc attachment in the nozzle.

To monitor the effects of steady state operation on starting phenomena, the test was run in four phases. At the end of the fourth phase performance measurements were taken and two additional tests were performed. These are summarized in Table 1. Each phase consisted of a number of short starts (typically 5 to 10 sec) and a burn-in period. Successive short starts were taken at approximately 3 min intervals. This was a compromise due to the time necessary to cool the thruster completely in the vacuum environment. As the first practical application of the arcjet thruster will probably involve the use of hydrazine propellant entering the thruster at an elevated temperature it was felt that the slight heating of the thruster body would not be detrimental to experimental results. Prior to the initial thruster assembly the cathode was weighed and photomicrographs of the cathode tip and scanning electron microscope (SEM) photographs of the anode were taken.

Phase I began with 42 short starts followed by a 10 min burn-in period. This was followed by 7 short starts. Little difference in starting phenomena was seen before and after the burn-in period so Phase II was completed before the thruster was disassembled for inspection and documentation. This and following documentation periods involved the same measurements taken prior to Phase I. Phase II consisted of 7 short starts and a 30 min burn-in period followed by 10 short starts. In Phase III, 20 short starts preceded and followed a 1 hr burn-in period. Once again the thruster was disassembled for documentation. Phase IV consisted of 28 short starts, a 10 hr burn-in period and 32 more short starts. After a final disassembly for documentation the thruster was reassembled for performance testing and to bring the total number of starts to more than 300. Finally, two further tests were run to examine starting phenomena. In each the thruster was reassembled with a newly polished cathode. In the first test, the thruster was subjected to 30 brief starts, none longer than 15 sec in duration. In the second the thruster was started once and run for 30 min.

Results and Discussion

As indicated in the preceding section, the test was performed in four phases; followed by performance measurements and two brief special tests. Each phase entailed a number of short starts and a burn-in period. The burn-in period was lengthened in each successive phase in order to observe the effect of steady state operation on starting phenomena. A more complete discussion of the starting conditions and quality is given elsewhere.[16] As the Phase I burn-in period was brief and the voltage and current traces were similar in starts before and after the burn-in, it was decided to perform Phase II before the first disassembly for inspection. The thruster was disassembled for inspection again after Phases III and IV. The following details the changes in the condition of the electrodes with time and presents, where possible, a discussion of the physical processes responsible for these changes.

A photomicrograph of the cathode tip as it went into the initial assembly is shown in Fig. 4. The tip was first ground to a half-angle of roughly 30° and then polished further in an attempt to remove the sharp shoulders and rough edges produced in the grinding process. This was done in an effort to decrease the probability of arc initiation upstream of the cathode tip. The final half-angle was measured to be 25°.

The anode had been reconditioned after a prior test. SEM photographs of the upstream (chamber) side of the insert are shown in Fig. 5. Figure 5(a) shows the interior surface to be clean and free of machining burrs near the constrictor entrance. Small cracks that run the length of the constrictor were noticeable at approximately 60° intervals. These cracks are due to thermal stresses and have been a common observation in tests of low power, constricted-arc arcjet thrusters at NASA Lewis and at the Rocket Research Company.[17] Though the appearance of these cracks, and the fact that they have proven unavoidable to date, were initially a cause for concern, extended testing has shown no evidence that they are performance or life limiting. A highly magnified view of one of these is shown in Fig. 5(b). The nozzle side of the anode was similar in appearance with the exception of a burr on the lip of the constrictor exit. This burr was left in place to act as an indicator of heat load in this region of the anode throughout the test.

Examination of the cathode after Phase II showed both a change in the appearance of the conical surface leading to the shoulder of the cathode and a recession of the tip. Figure 6 shows photomicrographs of the conical surface with Fig. 6(a) taken near the tip and Fig. 6(b) taken nearer the shoulder. From these it is obvious that the entire conical surface was roughened by surface melting. The melting was more pronounced near the tip. Upstream of the shoulder there was no change from the original condition. To determine whether this melting was due to starting phenomena or simply a lack of sufficient conductive and convective cooling during steady state operation, two separate tests were performed after Phase IV and the performance testing. In the first test, the thruster was assembled with a newly polished cathode and thirty brief starts (approximately 15 sec) were run. The tip of this cathode displayed the same molten appearance as described above. In the second test, the thruster was assembled once again with a polished cathode. This time the thruster was started once and run continuously for 30 min. Upon inspection this cathode did not show the roughened appearance noted in the previous test. From this it is apparent that the melting is related to a starting phenomena. It is likely that the arc originates behind the cathode tip and moves rapidly over the surface before reaching a stable operating point at the tip. This behavior has been previously noted.[18]

Photomicrographs taken from directly above the cathode tip at the conclusion of Phases II, III, and IV show that the entire tip was molten during operation. By the end of Phase II, the cathode had

recessed from its original geometry to a nearly circular plateau approximately 0.3 mm in diameter. This change in geometry is illustrated in Fig. 7(a). Two distinct regions were obvious, an inner depression roughly conical in shape and about 0.16 mm in diameter and an outer molten ring. Closer examination of the inner region showed there were a series of small rings leading to the bottom of the crater. The crater was slightly offset from the cathode centerline. Basically the same appearance was seen after Phase IV and this is shown in Fig. 7(b). After Phase III, no central crater was observed. Rather, the entire tip was crater shaped and approximately one fourth of the molten area was roughened as if it had recrystallized differently than the other area. Weighings after each phase indicated that no material (to the accuracy of one milligram) had been lost from the cathode. Little difference was noted in the diameters of the molten area from phase to phase. This indicates that the cathode tip rapidly reaches an equilibruim condition during steady state operation. From the aforementioned observations, and previous tests, it appears that a molten tip is unavoidable when thoriated tungsten is the cathode material. Also, it appears that the arc attaches in a small conical crater on the molten tip. This crater is usually apparent after resolidification of the tip once the arc is extinguished. That this was not seen after Phase III is probably due to the fact that the cathode was slightly misaligned during this period. This misalignment, documented in Ref. 16, probably caused the arc crater to set at an angle to the tip surface. If this were the case, the crater would be expected to collapse at the end of the run. The gross redistribution of material, even at the relatively low 10 A current level used in these tests, suggests that efforts to strongly affect the steady state operating geometry of the tip will not prove worthwhile. Some preshaping, to remove the excess material that becomes the outer molten ring, may be effective in reducing the amount of variation in tip geometry from the initial to the steady-state condition.

The condition of the converging side of the anode/nozzle insert after Phase II is shown in Fig. 8. Under low magnification, Fig. 8(a), both an extensive network of stress cracks and darkened swirl marks in the direction of the flow pattern are apparent. Higher magnification near the constrictor (Fig. 8(b)) shows that surface melting had occurred. A thin raised surface with a roughened, crystalline appearance covered much of the area. In some spots this surface layer had formed into larger deposits (tungsten beads and ridges approximately 10 μm in diameter - see Fig. 8(b)) leaving a relatively clean surface. Less surface melting was evident farther upstream of the constrictor. The swirl marks indicate that the arc initiates upstream of the cathode tip and on the converging surface of the anode before it is forced to its steady-state position by the flowfield. Away from the edge of the constrictor the surface covered by the tracks showed no more melting than adjacent, untracked surfaces, so arc motion must be rapid. The exact nature of the darkening is under investigation. Melting was also apparent at the entrance to the constrictor. This was a localized phenomenon as it was very obvious on one part of the edge while the other was basically untouched as shown in Fig. 8(c). The side on which the melting occurred also corresponds to the side on which the darkest arc tracks end.

It is evident that the arc initiates upstream of the cathode tip between the conical side of the cathode and the converging side of the anode before moving to its steady state position. From the appearance of the molten area at the constrictor entrance it is also evident that the anode spot attaches at this point before traversing the length of the constrictor to the exit. The reason for the preferential attachment, shown in Fig. 8(c), is still under investigation but is likely due to electrode misalignment problems caused by the small dimensional tolerance near the constrictor entrance. During Phases III and IV the melting become more extensive as shown in Figs. 9 and 10, respectively. After Phase III much of the constrictor was still relatively clean, but molten material had appeared near many of the cracks. This could indicate that the cracks are regions of high electric field strength that influence arc attachment, but further investigation is required before this conclusion could be drawn with certainty. After Phase IV, there was some molten material around most of the constrictor entrance. Still, some portions of the entrance were less affected than others. From the evidence gathered to this point it is postulated that electrode alignment influences the path the anode spot takes, but that there is also some degree of randomness involved in this transition process.

Unlike the chamber side of the anode, the nozzle side showed no evidence of melting. SEM photographs of the area near the constrictor and the constrictor from the nozzle side taken after Phases II, III, and IV are shown in Figs. 11, 12, and 13, respectively. With the exception of a lengthening of the stress cracks there was virtually no change in the appearance of the nozzle side from the initial assembly to the end of Phase II. Machining burrs on the lip of the exit were still clearly visible at this point. The only difference in appearance between Phases II and III was the appearance of a small sphere of molten tungsten near one of the stress cracks. The burr on the lip was still clearly visible behind this, and similar beads were visible inside the constrictor. This material is obviously being blown down the constrictor from the entrance. At the end of Phase IV more material was observed at the exit of the constrictor. Once again it is clear, from the presence of the burr, that this material is not due to any melting in the nozzle. These photographs are strong evidence that there is no spot mode attachment in the constrictor or diverging section of the nozzle during steady state operation. Spot attachment upstream in the high pressure region produced a significant amount of melting, and this decreased over the length of the constrictor. Were spot attachment occurring in the nozzle, it would be highly unlikely that the entire surface, including the sharp edges on the burrs and stress crack edges, would completely escape melting.

Concluding Remarks

The arcjet/power supply combination used in this test appears to have eliminated the sustained low mode operation observed in previous studies as 300 starts were reliably accomplished. This indicates that the number of starts anticipated in an actual satellite application should not present a problem. Still, a full, cycled life test will probably be necessary to completely eliminate starting concerns.

At the current level used in this study, severe erosion of the cathode tip is not expected to be a life-limiting issue. As expected, a molten tip was found to be unavoidable during steady-state operation, but it was also found that recession of the tip to a steady state operating geometry occurred rapidly and with no apparent material loss. It appears that some material could be removed from the cathode tip prior to operation to reduce the variation in geometry from the initial to the steady-state conditions.

Close examination of the electrodes as the test progressed indicates that the arc strikes, initially, between a point upstream of the cathode tip and the interior converging surface of the anode. While the transition to the steady state occurred rapidly and caused no cathode-related problems, melting at the entrance to the constrictor was observed. Although this was not as severe as that seen in earlier studies and did not appear to be performance limiting it, is a cause of concern as it worsened with time and number of starts. The localized nature of the melting is indicative of alignment problems, and this suggests that future efforts to increase starting reliability and lessen the extent of anode damage should be directed towards improvement in electrode alignment. This could entail a change in assembly procedure, an improvement in machining tolerances or a combination of these.

Finally, the absence of melting in the nozzle region of the anode implies that diffuse, rather than spot, mode attachment occurs when the arc stabilizes and seats in this area.

References

1. Wallner, L.E. and Czika, J., Jr., "Arcjet Thrustor for Space Propulsion," NASA TN D-2868, 1965

2. "Arc-Jet Application Study," General Electric Co., Cincinnati, OH, Sept. 1961, (NASA CR-140076).

3. John, R.R., Connors, J.F., and Bennett, S., "Thirty Day Endurance Test of 30 KW Arcjet Engine," AIAA Paper 63-274, June 1963.

4. John, R.R., "Thirty Kilowatt Plasmajet Rocket-Engine Development," Avco Corp., Wilmington, MA, RAD-TR-4-6, July 1964. (NASA CR-54044).

5. Todd, J.P. and Sheets, R.E., "Development of a Regeneratively Cooled 30-KW Arc Jet Engine," AIAA Journal, Vol. 3, No. 1, Jan. 1965, pp. 122-126.

6. Todd, J.P., "30 KW Arc-Jet Thrustor Research," Giannini Scientific Corp., APL-TDR-64-58, Mar. 1964.

7. Ducati, A.C. Humpal, H., Meltzer, J., Muehlberger, E., Todd, J.P., and Waltzer, H., "1-KW Arc Jet-Engine System Performance Test," Journal of Spacecraft, Vol. 1, No. 3, May-June 1964, pp. 327-332.

8. Greco, R.V., and Stoner, W.A., "Development of a Plasmajet Rocket Engine for Attitude Control," Plasmadyne Corp., GRC-1341-A, Dec. 1961.

9. McCaughey, O.J., Geideman, W.A., Jr., and Muller, K., "Research and Advanced Development of a 2 KW Arc-Jet Thrustor," Plasmadyne Corp. Santa Ana, CA, GRC-1646, 1963, (NASA CR-54035).

10. Hardy, T.L., Rawlin, V.K., and Pattern, M.J., "Electric Propulsion Options for the SP-100 Reference Mission," NASA TM 88918, 1987.

11. Pivirotto, T., King, D., Deininger, W., and Brophy, J., "The Design and Operating Characteristics of a 30 KW Thermal Arciet Engine for Space Propulsion," AIAA Paper 86-1508, June 1986.

12. Knowles, S.C., Smith, W.W., Chun, S.I., and Feconda, R.T., "Low Power Hydrazine Arcjets": A System Description for Near-Term Application, 1986 JANNAF Propulsion Meeting, New Orleans, LA; August 1986.

13. Nakanishi, S., "Performance Evaluation of a 1 KW Arc Jet Thruster," AIAA Paper 85-2033, Oct. 1985.

14. Curran, F.M. and Nakanishi, S., "Low Power dc Arcjet Operation with Hydrogen/Nitrogen Propellant Mixtures," NASA TM-87279, June 1986.

15. Gruber, R.P., "Power Electronics for a 1-Kilowatt Arcjet Thruster," AIAA Paper 86-1507, June 1986.

16. Haag, T.W. and Curran, F.M., "Arcjet Starting Reliability: A Multistart Test on Hydrogen/Nitrogen Mixtures," AIAA-87-1061, to be presented at the 19th AIAA/DGLR/JSASS International Electric Propulsion Conference, Colorado Springs, CO, May 1987.

17. Knowles, S.K. and Smith, W.W., Private communications, Rocket Research Co., Redmond, WA, 1986.

18. Sarmiento, C.: Private communication, NASA Lewis Research Center, Cleveland, OH, 1987.

TABLE I. - STARTING RELIABILITY TEST SEQUENCE

	Phase I	Phase II	Phase III	Phase IV	Extended operation
Initial starts	42	7	20	28	92
Burn-in period	10 min	30 min	1 hr	10 hr	2 hr of performance testing + 2 extra tests
Final starts	7	10	20	32	16
Disassembly/ inspection	No	Yes	Yes	Yes	No

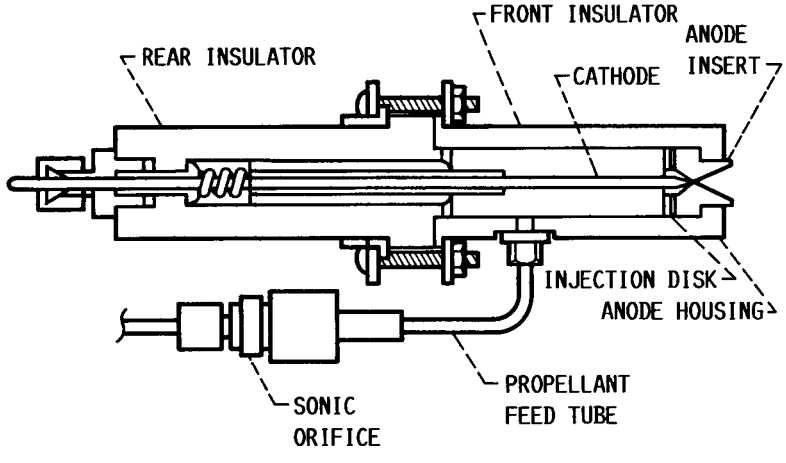

(A) CROSS SECTIONAL SCHEMATIC OF ARCJET.

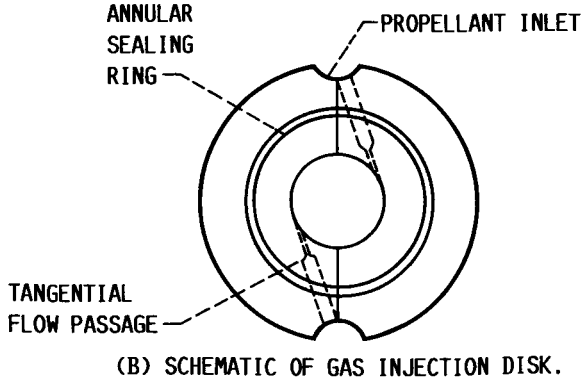

(B) SCHEMATIC OF GAS INJECTION DISK.

FIGURE 1. - ARCJET SCHEMATIC DIAGRAMS.

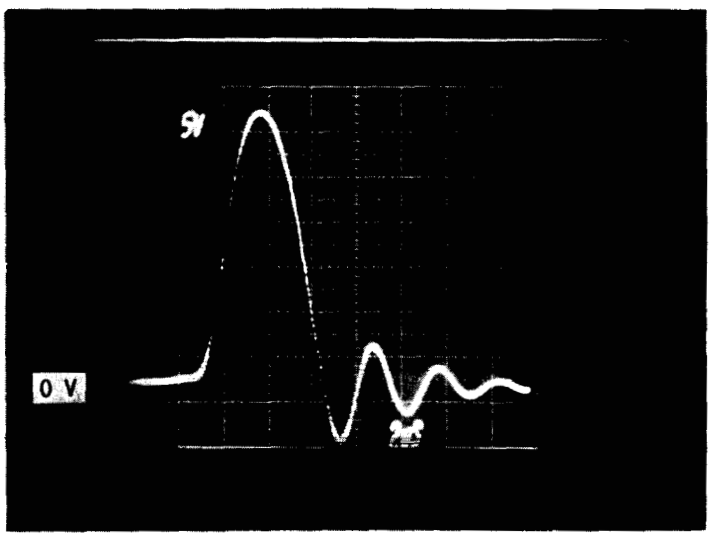

FIGURE 2. - OPEN-CIRCUIT STARTING PULSE. SCALE:
VERTICAL - 500 V/DIVISION, HORIZONTAL - 2 µs/DIVISION.

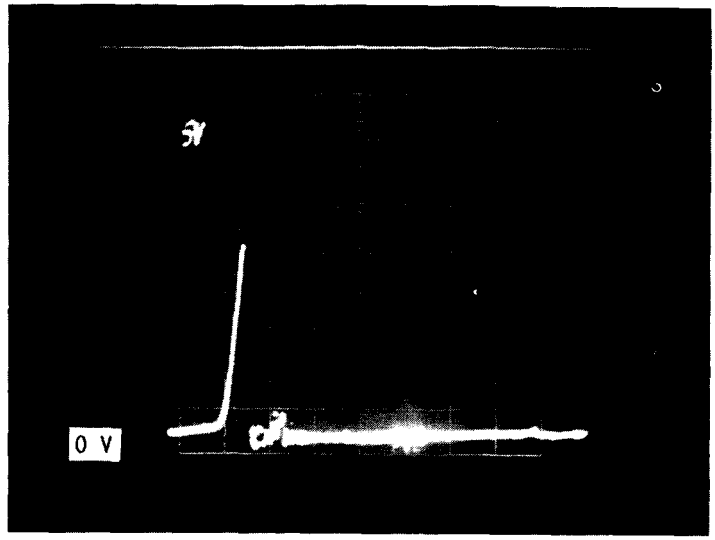

(A) A STARTUP WITH NO VOLTAGE OSCILLATIONS.

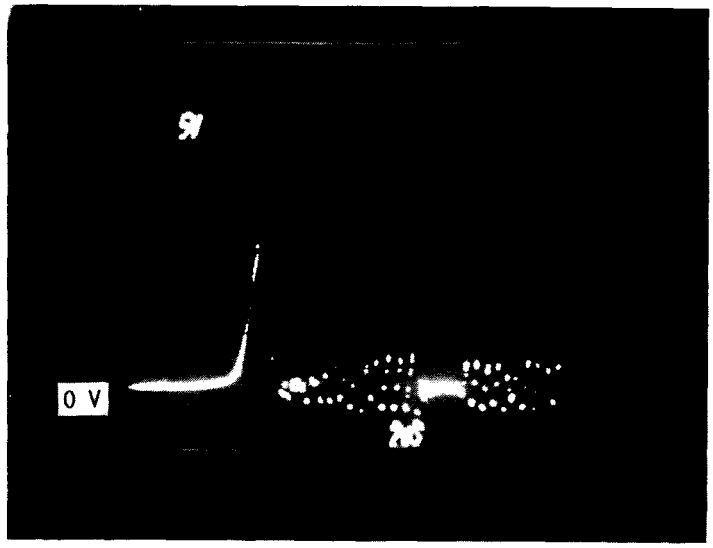

(B) A STARTUP WITH VOLTAGE OSCILLATIONS.

FIGURE 3. - OSCILLOSCOPE PHOTOGRAPHS OF TYPICAL STARTING TRANSIENTS. SCALE: VERTICAL - 500 V/DIVISION, HORIZONTAL - 2 μs/DIVISION.

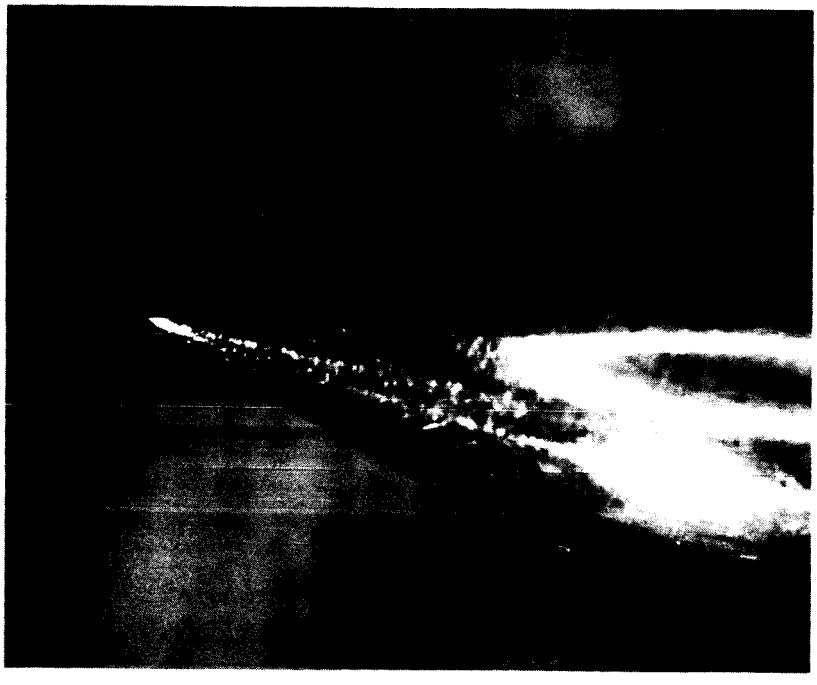

FIGURE 4. - CATHODE TIP PROIR TO TEST (15x).

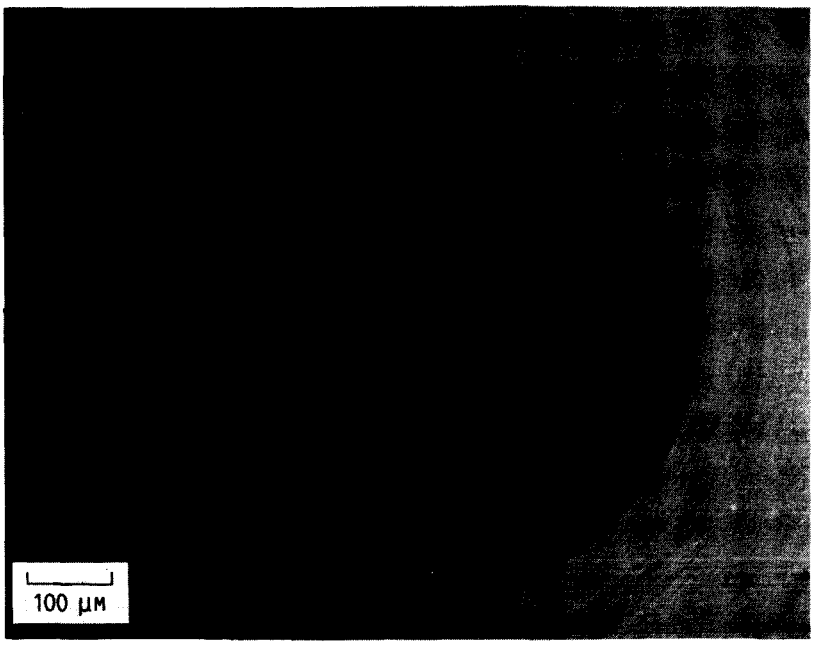

(A) CONSTRICTOR ENTRANCE (110x).

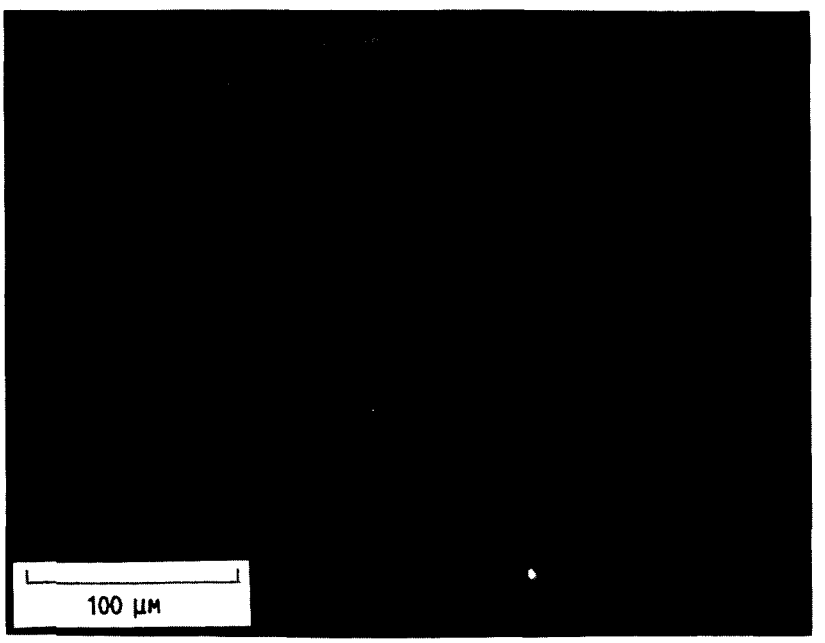

(B) CLOSE UP OF STRESS CRACK (280x).

FIGURE 5. - CHAMBER SIDE OF ANODE PRIOR TO TESTING.

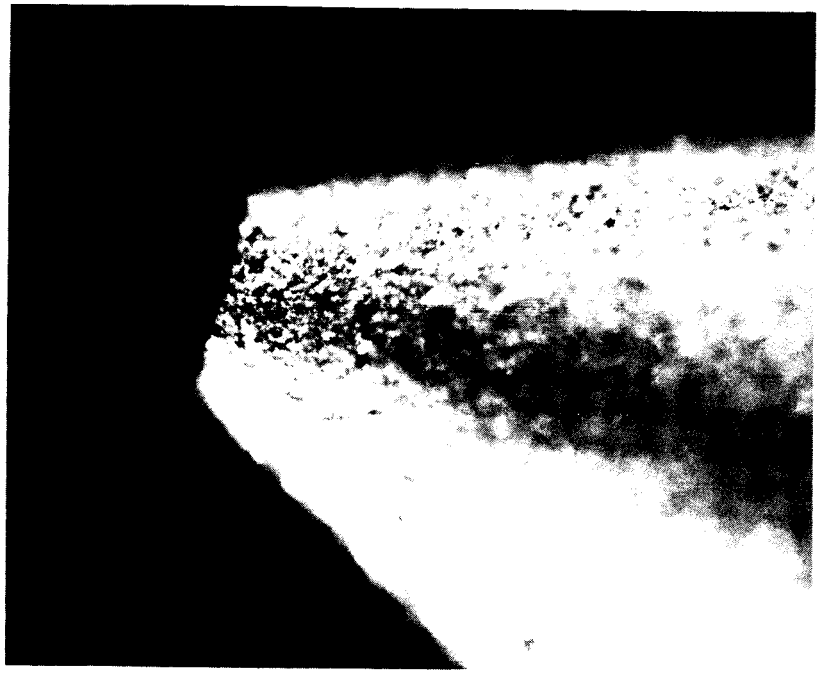

(A) SIDE VIEW OF CATHODE NEAR TIP (80x).

(B) SIDE VIEW OF CATHODE NEAR SHOULDER (80x).

FIGURE 6. - PHOTOMICROGRAPHS OF CATHODE SIDE NEAR TIP AFTER PHASE II.

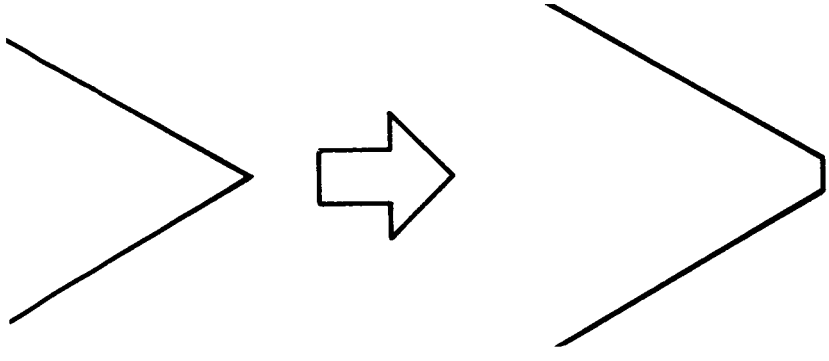

(A) CROSS-SECTIONAL SCHEMATIC OF CATHODE TIP RECESSION TO THE STEADY STATE OPERATING CONDITION (I.E. AFTER PHASE II, III, AND IV.

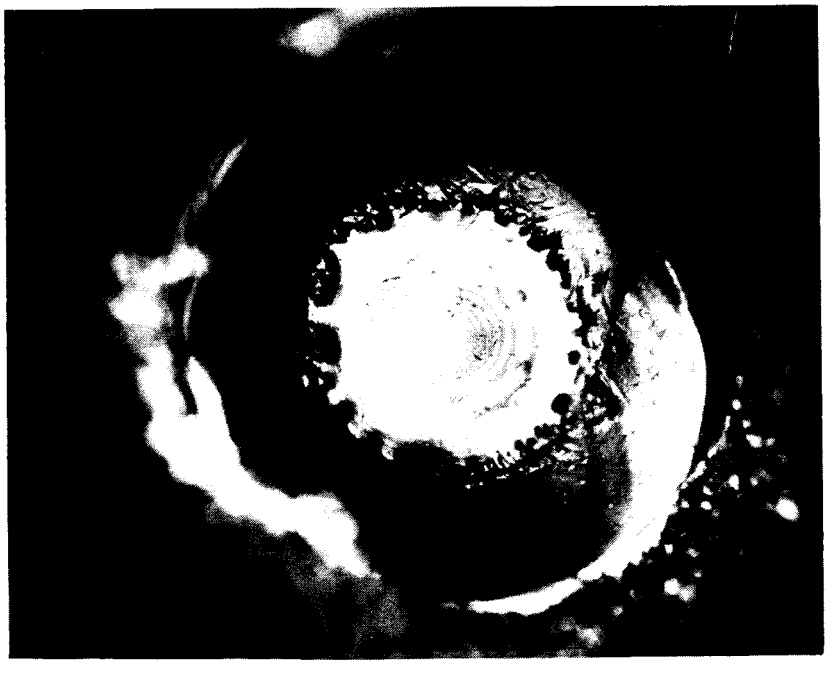

(B) PHOTOMICROGRAPH OF CATHODE TIP AFTER PHASE IV (200x).

FIGURE 7. - CATHODE TIP AFTER EXTENDED OPERATION.

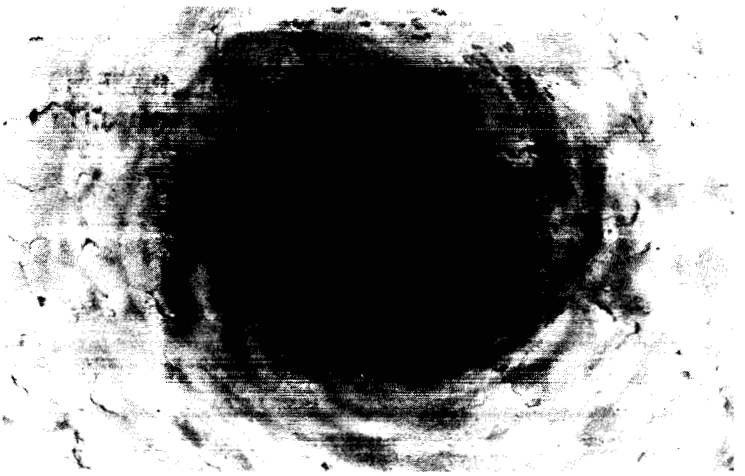

(A) CHAMBER SIDE OF ANODE (50x).

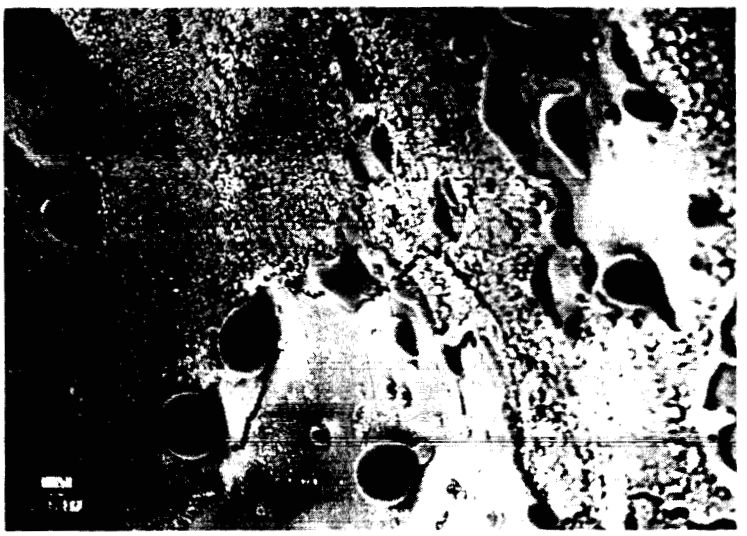

(B) HIGHLY MAGNIFIED VIEW OF SURFACE NEAR THE CONSTRICTOR (500x).

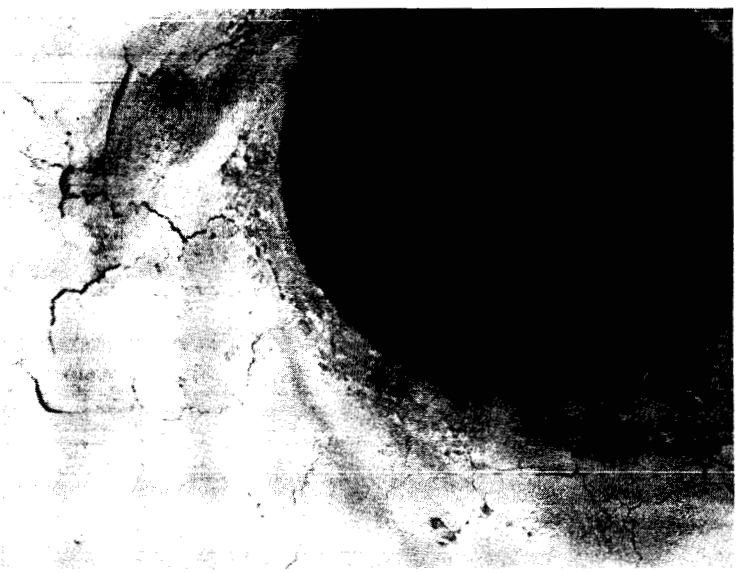

(C) CONSTRICTOR ENTRANCE (120x).

FIGURE 8. - SEM PHOTOGRAPHS OF CHAMBER SIDE OF THE ANODE AFTER PHASE II.

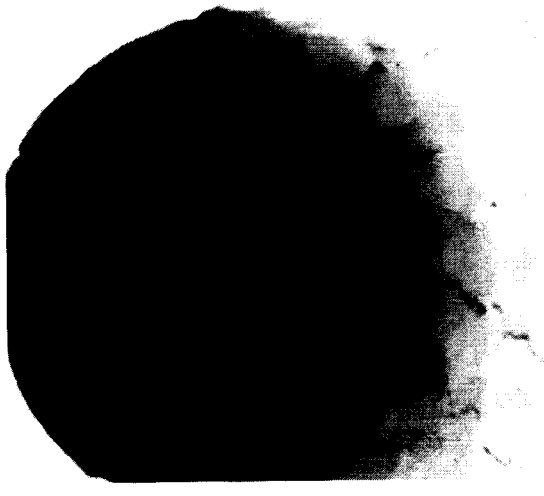

(A) CHAMBER SIDE OF ANODE (110x).

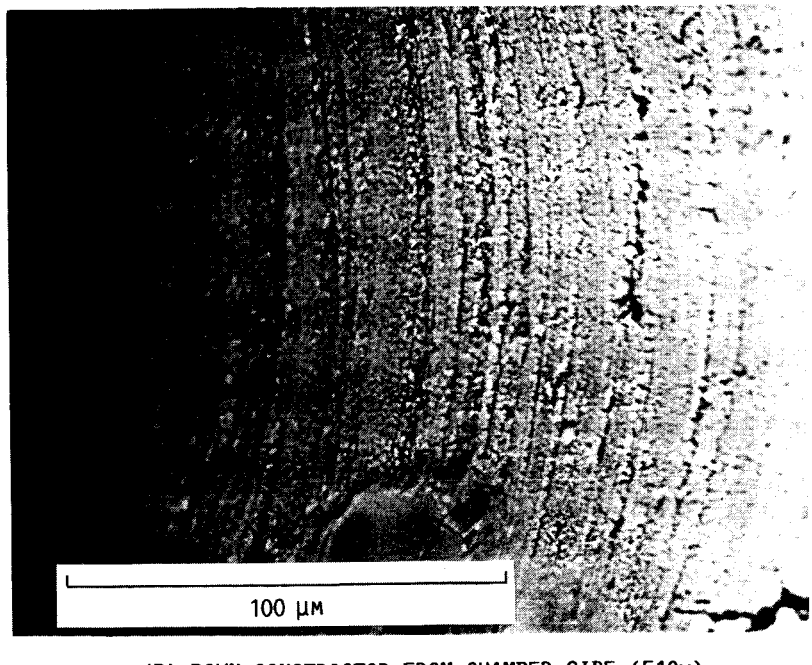

(B) DOWN CONSTRICTOR FROM CHAMBER SIDE (510x).

FIGURE 9. - SEM PHOTOGRAPH OF CHAMBER SIDE OF ANODE AFTER PHASE III.

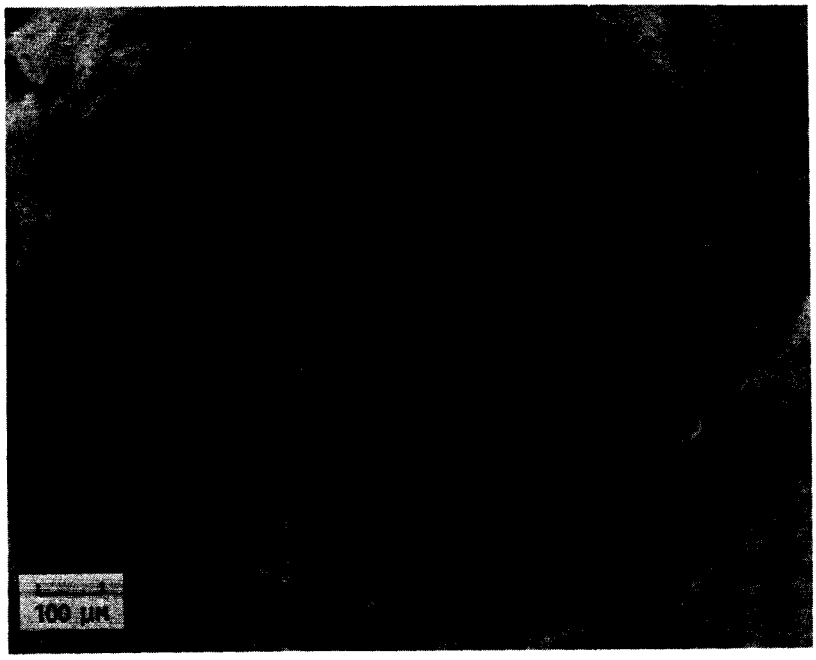

(A) CHAMBER SIDE OF ANODE (90x).

(B) CONSTRICTOR FROM CHAMBER SIDE (160x).

FIGURE 10. - CHAMBER SIDE OF ANODE AFTER PHASE IV.

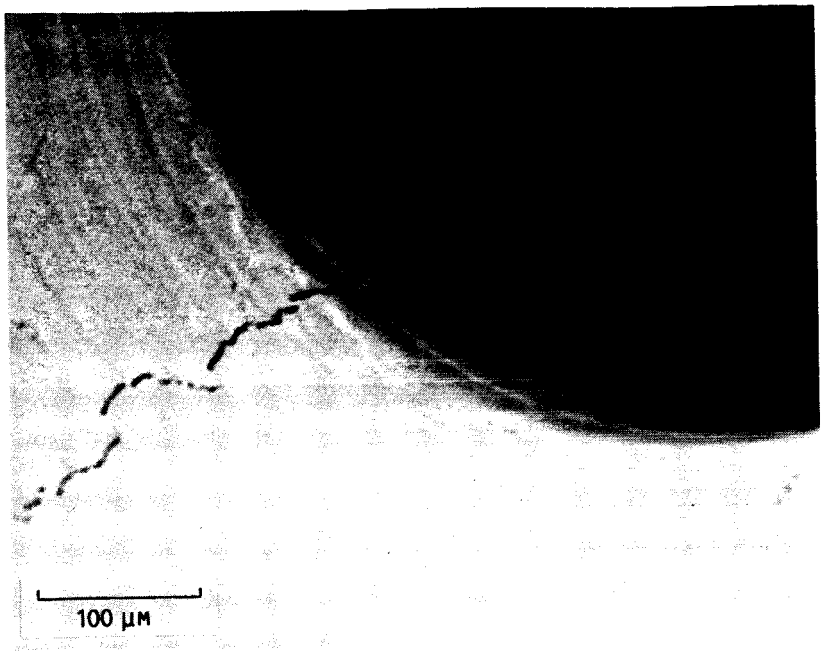

(A) NOZZLE SIDE OF ANODE (80x).

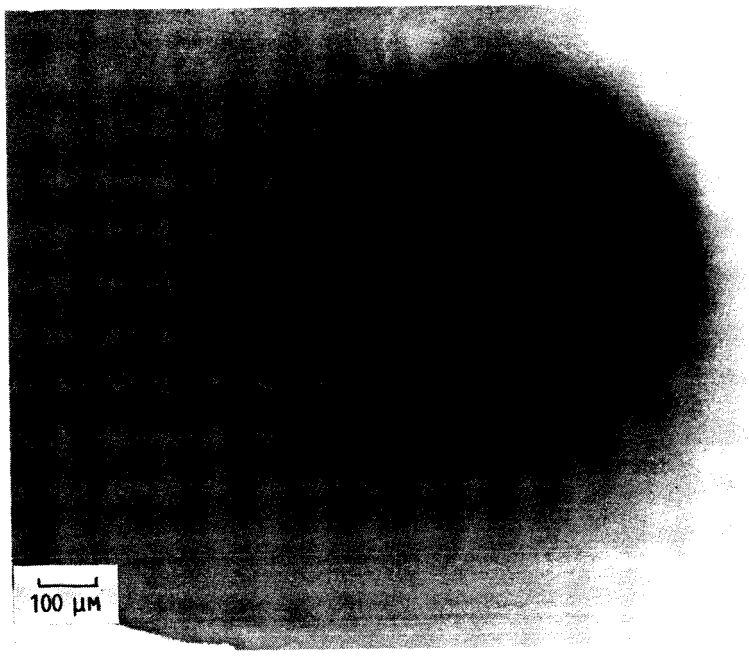

(B) CONSTRICTOR FROM NOZZLE SIDE (220x).

FIGURE 11. - SEM PHOTOGRAPHS FROM NOZZLE SIDE OF ANODE AFTER PHASE II.

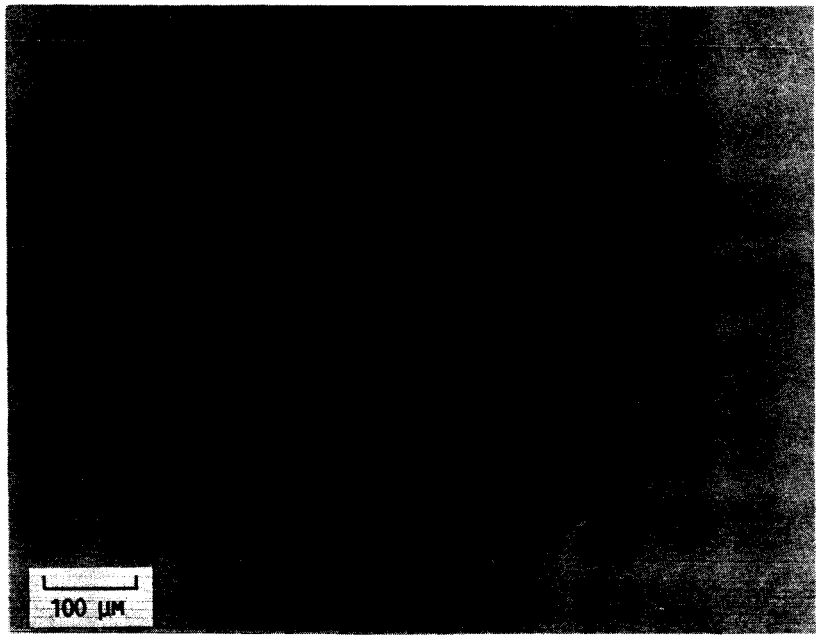

(A) CONSTRICTOR FROM NOZZLE SIDE (120x).

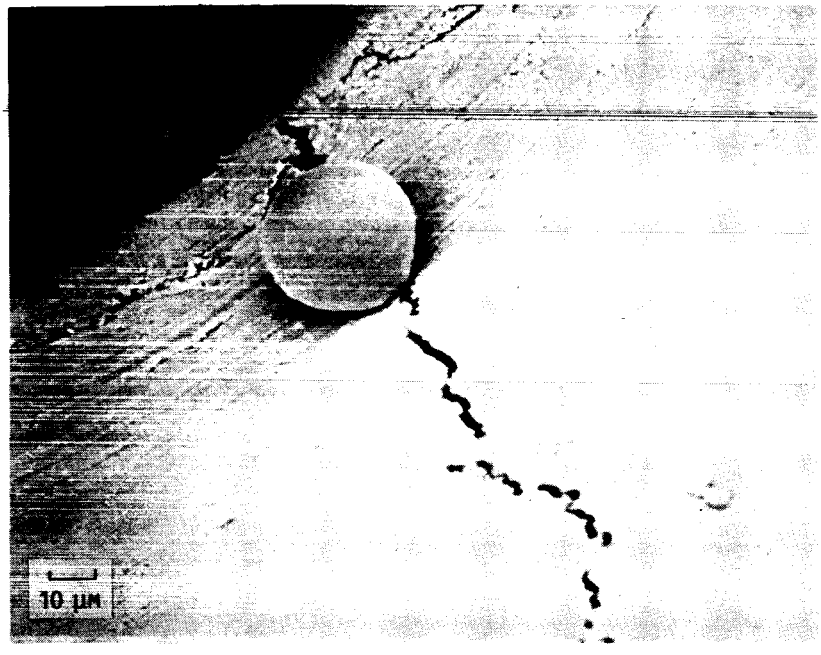

(B) CONSTRICTOR LIP FROM NOZZLE SIDE (600x).

FIGURE 12. - SEM PHOTOGRAPHS FROM NOZZLE SIDE OF ANODE AFTER PHASE III.

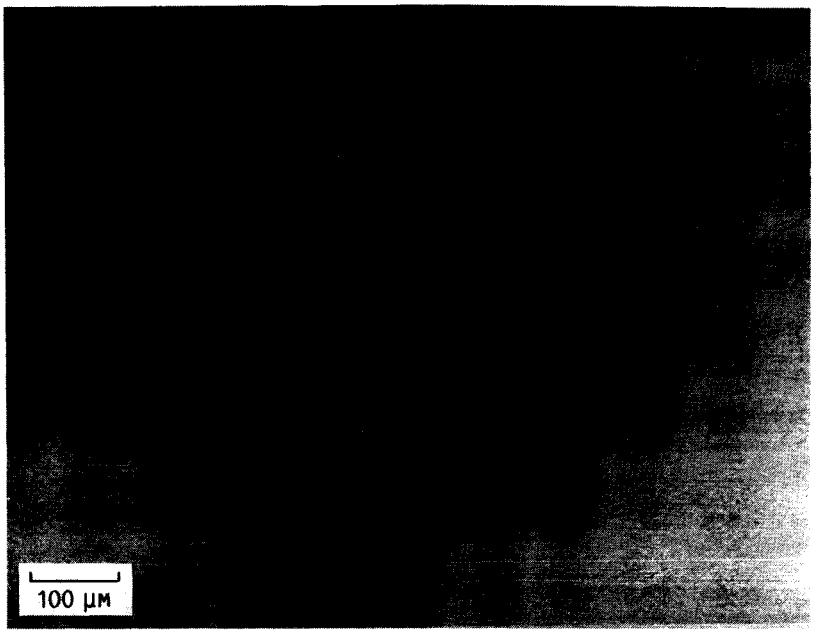

(A) CONSTRICTOR FROM NOZZLE SIDE (110x).

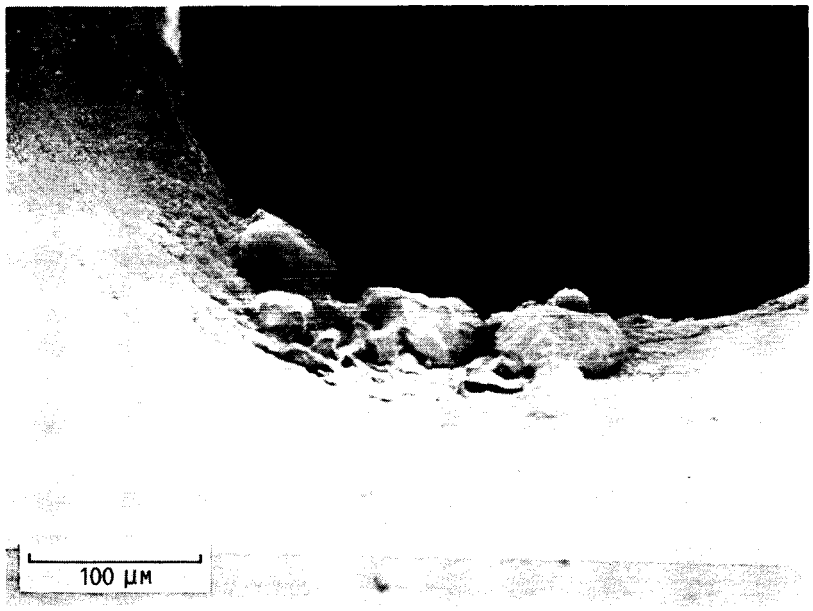

(B) CONSTRICTOR TIP FROM NOZZLE SIDE (210x).

FIGURE 13. - SEM PHOTOGRAPHS OF ANODE FROM NOZZLE SIDE AFTER PHASE IV.

1. Report No. NASA TM-89857 AIAA-87-1060	2. Government Accession No.	3. Recipient's Catalog No.
4. Title and Subtitle Arcjet Component Conditions Through a Multistart Test		5. Report Date 6. Performing Organization Code 506-42-31
7. Author(s) Frank M. Curran and Thomas W. Haag		8. Performing Organization Report No. E-3525 10. Work Unit No.
9. Performing Organization Name and Address National Aeronautics and Space Administration Lewis Research Center Cleveland, Ohio 44135		11. Contract or Grant No. 13. Type of Report and Period Covered Technical Memorandum
12. Sponsoring Agency Name and Address National Aeronautics and Space Administration Washington, D.C. 20546		14. Sponsoring Agency Code

15. Supplementary Notes

Prepared for the 19th International Electric Propulsion Conference cosponsored by the AIAA, DGLR, and JSASS, Colorado Springs, Colorado, May 11-13, 1987.

16. Abstract

A low power, dc arcjet thruster was tested for starting reliability using hydrogen-nitrogen mixtures simulating the decomposition products of hydrazine. More than 300 starts were accumulated in phases with extended burn-in periods interlaced. A high degree of flow stabilization was built into the arcjet and the power supply incorporated both rapid current regulation and a high voltage, pulsed starting circuit. A nominal current level of 10 A was maintained throughout the test. Photomicrographs of the cathode tip showed a rapid recession to a steady-state operating geometry. A target of 300 starts was selected, as this represents significantly more than anticipated (150-240), in missions of 10 yr or less duration. Weighings showed no apparent mass loss. Some anode erosion was observed, particularly at the entrance to the constrictor. This was attributed to the brief period during startup the arc mode attachment point spends in the high pressure region upstream of the nozzle. Based on the results obtained, startup does not appear to be performance or lifelimiting for the number of starts typical of operational satellite applications.

17. Key Words (Suggested by Author(s))	18. Distribution Statement
Arcjet; Auxiliary propulsion; Electric propulsion	Unclassified - unlimited STAR Category 20

19. Security Classif. (of this report)	20. Security Classif. (of this page)	21. No. of pages	22. Price*
Unclassified	Unclassified		

*For sale by the National Technical Information Service, Springfield, Virginia 22161